Solvolysis Depolymerization of Additive-Containing Poly(lactic Acid) Composites for Sustainable Ethyl Lactate Production

Eva Domincova Bergerova[1*], Jaroslav Cisar[1], Monika Strasakova[1], Simona Uhercova[1], Dominika Hanusova[1], Miroslava Dusankova[1], David Skoda[1], Vladimir Sedlarik[1]

[1]Centre of Polymer Systems, University Institute, Tomas Bata University in Zlin, tr. Tomase Bati 5678,760 01 Zlin, Czech Republic

*Corresponding author: Eva Domincova Bergerova, domincova_bergerova@utb.cz

Abstract

The increasing use of poly(lactic acid) materials has led to growing amounts of post-consumer waste containing commonly used industrial additives that complicate end-of-life treatment. Although solvolysis represents a promising chemical recycling route for PLA, systematic comparative data quantifying the influence of common additives under relatively mild reaction conditions remain scarce. This study investigates the solvolysis depolymerization of PLA-based composites containing typical additives, including calcium carbonate (1–10 wt %), carbon black, plasticizers, cellulose, and minor polymeric components. Depolymerization was performed in an acetone/ethanol system at 70 °C using the organocatalyst 1,5,7-triazabicyclo[4.4.0]dec-5-ene, enabling recovery of ethyl lactate as a bio-based solvent.

Depolymerization efficiencies ranged from 61-100 %, depending on additive form and content. High efficiencies and PLA conversion to ethyl lactate (up to 98%) were obtained for materials containing low amounts of inorganic additives (≤2 wt%), whereas cellulose-rich composites showed markedly reduced degradation and product formation. The results demonstrate that additive form and content govern depolymerization performance more strongly than crystallinity effects alone, with cellulose-rich matrices (>50 wt%) defining a practical compositional threshold for efficient chemical recycling. Structural and thermal analyses (GPC, DSC, TGA, and XRD) indicated that additives increased crystallinity and thermal stability while solvolysis remained effective at low to moderate additive loadings. This work extends solvolysis recycling strategies from virgin PLA to commercially relevant composite materials and defines compositional limits for efficient ethyl lactate production from additive-containing PLA waste.

Keywords: poly(lactic acid); industrial additive; chemical recycling; solvolysis; ethyl lactate; composites

1. Introduction

The increasing demand for sustainable polymeric materials has led to the widespread use of poly(lactic acid) (PLA), particularly in packaging, agriculture, and technical applications [1–3]. In industrial practice, PLA is rarely used as a neat polymer but is typically formulated as a composite containing mineral fillers, plasticizers, pigments, fibers, or secondary polymers to improve mechanical performance, thermal stability, and processability [4–18]. As a result, most commercially available PLA products and post-consumer waste streams consist of multi-component, additive-containing composite materials rather than virgin PLA.

The production of PLA is associated with a cumulative energy demand of approximately 50–60 GJ t^{-1} (14–17 MWh t^{-1}), depending on the production route and system boundaries. When additional processing steps such as melt extrusion into filaments or films are included, the total energy demand for finished PLA products can reach 54–79 GJ t^{-1} (15–22 MWh t^{-1}) [19,20]. This embedded energy is irreversibly lost during biodegradation of PLA. In contrast, solvolysis enables recovery of ethyl lactate, whose conventional synthesis from lactic acid requires more than 30–40 GJ t^{-1} (8–11 MWh t^{-1}) [21], highlighting the potential energy advantage of chemical recycling over both composting and virgin solvent production.

Mechanical recycling of PLA composites is technologically simple but suffers from significant drawbacks, including chain scission, molecular weight reduction, deterioration of mechanical properties, and poor dispersion of fillers upon repeated processing, resulting in limited recyclate quality and low recycling rates [22–26]. Composting is often presented as an end-of-life option for PLA; however, its practical applicability remains limited due to insufficient industrial composting infrastructure and strict processing requirements, particularly for additive-containing composite materials. Moreover, composting leads to irreversible loss of the material value and embedded energy, as the polymer is converted into CO_2, water, and biomass [27–31].

Accordingly, chemical recycling has emerged as a more controllable and resource-efficient strategy for managing PLA waste within a circular economy framework. Depolymerization enables conversion of PLA into value-added products such as ethyl lactate, a bio-based solvent with low toxicity, biodegradability, and favourable solvency properties [4,32,33]. However, the practical feasibility of chemical recycling critically depends on its performance in additive-containing PLA waste streams, which dominate real post-consumer materials.

Selective chemical depolymerization, particularly solvolysis, has therefore attracted increasing attention as a promising approach for recovering high-value products [33–36]. Solvolysis offers efficient depolymerization under relatively mild conditions, high product purity, and compatibility with circular economy principles [37–39]. Nevertheless, most published studies focus on neat PLA or simplified laboratory systems. Systematic investigations addressing industrially relevant, additive-rich PLA composites under comparable reaction conditions remain scarce, representing a critical knowledge gap.

In our previous work [40], we demonstrated that the solvolysis depolymerization of virgin PLA is strongly governed by polymer architecture and crystallinity. Building on these findings, the present study addresses a critical knowledge gap by focusing on PLA composite materials representative of industrial practice. Specifically, composites containing calcium carbonate, carbon black, plasticizers, cellulose, and secondary polymers were selected, as these additives are widely used in commercial PLA products to tailor cost, stiffness, thermal behavior, coloration, and processability [4–9,11–18]. To date, a systematic evaluation of how such additive-rich PLA composites behave under comparable and well-controlled reaction conditions has not been comprehensively reported in the literature.

The aim of this work is to systematically evaluate the impact of additive form and content on the solvolysis depolymerization efficiency of PLA composites and on ethyl lactate recovery under mild conditions, thereby defining practical compositional limits for efficient chemical recycling of industrial PLA materials. Solvolysis was performed in an acetone/ethanol system using an organocatalyst under comparable reaction conditions. By combining depolymerization experiments with structural and thermal characterization (GPC, DSC, TGA, and XRD), this study evaluates how material form and additive content influence PLA composite recyclability, providing insights to inform the design of robust solvolysis recycling strategies.

2. Materials and methods

2.1 Materials

Chemicals (acetone, ethanol, ethyl lactate standards, and TBD catalyst) were purchased from commercial suppliers and used as received, following the procedure described in our previous work [40]. These reagents were applied as received without further purification. Virgin (pure) PLA, of type Ingeo 2003D (PLA-A), M_w: 150 – 200 kDa ± 4000 Da, PI: 1.7-1.8, was used in the experiment to determine the extent of decomposition and to obtain the ethyl lactate product (Table 1). The PLA samples denoted B and C were prepared by the authors´

team [41]. PLA samples D–E were obtained from the specified sources; however, the manufacturer does not disclose the exact composition of the material. Therefore, the amount of additives was evaluated based on analyses conducted in our laboratory. Data on all tested material, including their composition, and producer, are given in Table 1.

Table 1 Overview of the tested PLA samples (original form), their composition and supplier

Sample	specification	sample composition	supplier
PLA-A	PLA granules	PLA Ingeo™ 2003D	NatureWorks®
PLA-B	PLA filaments	PLA + 1% $CaCO_3$ + (0.5%) CA	NatureWorks®/ own preparation
PLA-C	PLA foil	PLA + 10% $CaCO_3$ +(4%) plasticizer*	NatureWorks®/ own preparation
PLA-D	PLA woven stack	PLA + 1.5% $CaCO_3$ + (<1%) DETPE	Czech Fibre, CZ
PLA-E	PLA sackcloth	PLA + 1% $CaCO_3$ + (<1%) PBAT + (0,5%) CA	Juta, CZ
PLA-F	PLA laminate	PLA + 3.5% $CaCO_3$ + (<50%) cellulose	Oxalis, CZ

* plasticizer (copolymer PLA/PEG) – [41]

CA – carbon black

DETPE – diethyl-p-phthalate, PBAT - polybutylene adipate terephthalate

2.2 Experimental strategy

The experimental procedure was based on our previous work [40], with modifications as described below, with reaction conditions (acetone as solvent, ethanol as nucleophile, and TBD as catalyst at 70 °C). This approach was chosen deliberately to allow a direct comparison between the degradation behavior of virgin PLA reported earlier and the additive-rich composites studied here. Only the composition of the tested PLA materials differed, as detailed in Table 1.

The procedure for degradation of the polymer by alcoholysis was based on a transesterification reaction [32,33]. The depolymerization procedure followed our previous work [40], under mild reaction conditions (Scheme 1).

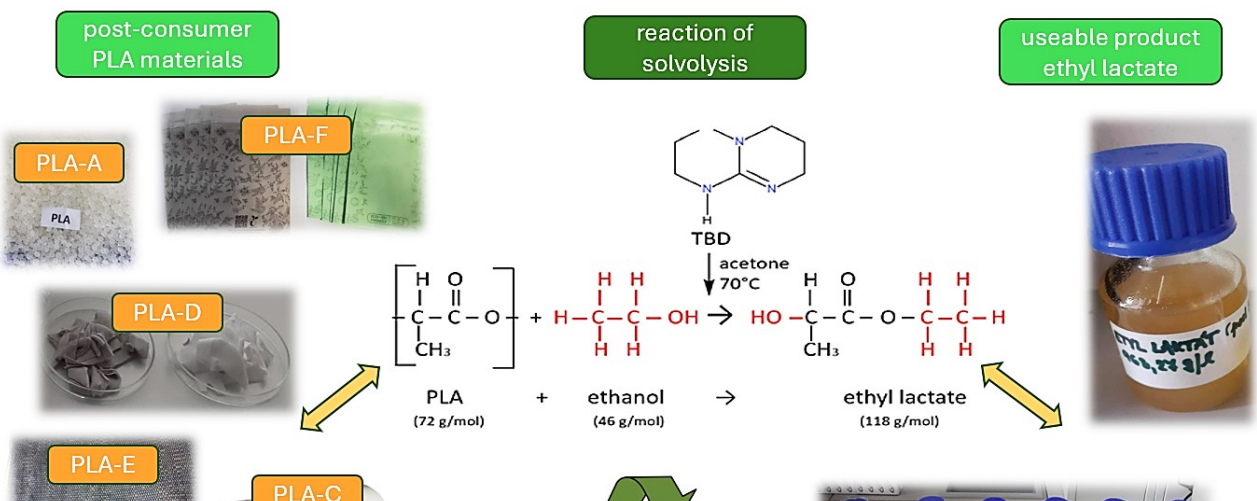

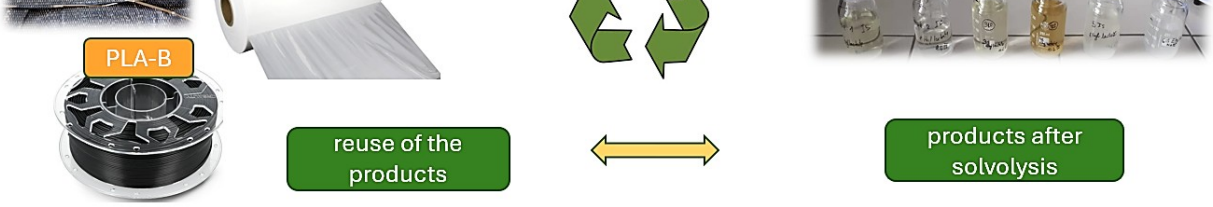

Scheme1 Environmentally friendly solvolysis of polylactic acid-based composite materials to ethyl lactate as a value-added product under comparable reaction mild conditions

This mixture was dissolved at 70°C for periods of 30 to 120 minutes, according to the character of sample, at the close of which the resultant solution was filtered through an Erlenmeyer flask.

Tests were conducted using 14.3 wt% PLA for the heavier PLA-A, PLA-B samples, and 4.04 wt% for the lighter PLA-C, PLA-D, PLA-E samples. The lower amount used for the latter samples was due to the bulky nature material, which made it impossible to introduce a larger quantity into the reaction flask. The samples were prepared using a solvent-to-nucleophile 1:2 and a catalyst amount of 2 wt% relative to the PLA mass. TBD, a bicyclic guanidine catalyst, was chosen for its selective and environmentally friendly characteristics, which align with the second, third, and eighth principles of green chemistry [32].

The degree of PLA decomposition was determined according to Equation *(1)* based on the mass balance of the initial and residual polymer. In addition, the conversion of PLA to ethyl lactate (EL) was calculated based on the amount of EL formed, assuming a one-to-one stoichiometry between the PLA repeating unit and ethyl lactate, as described by Equation *(2)* [40]. Additives such as carbon black and $CaCO_3$ remained on the filter together with the unreacted polymer matrix, while plasticizer passed into the filtrate.

The degree of PLA degradation (D_{PLA}) was determined by Equation 1:

$$D_{(PLA)} = \frac{w_0 - w_1}{w_0} x\ 100\,\%$$

(1)

where w_0 represents the initial amounts of PLA and w_1 represents the mass of the remaining unreacted PLA.

The conversion of PLA to EL (X_{PLA}) was calculated by Equation 2:

$$X_{(PLA)} = \frac{w_3}{w_0} x \frac{M(PLA)}{M(EL)} x\ 100\,\%$$

(2)

where w_0 represents the initial amounts of PLA, w_3 represents the mass of the ethyl lactate obtained, and $M_{(PLA)}$ = 72.06 g·mol^{-1} and $M_{(EL)}$ = 118.13 g·mol^{-1} are the molar masses of the PLA repeating unit and ethyl lactate, respectively.

It should be noted that $X_{(PLA)}$ was calculated based on the amount of ethyl lactate formed and therefore does not necessarily correspond to the gravimetrically determined $D_{(PLA)}$.

2.3 *Characterization of the end product and determination of PLA decomposition*

2.3.1 GC-FID

Gas chromatography with FID detector (GC-FID) was used to determine ethyl lactate concentration and purity under conditions identical to those previously described [43]. Samples were passed through a PTFE filter (0.22 µm) and diluted 10 times in methanol. Analysis was performed on a gas chromatograph (Shimadzu GC-2010 Plus, Kyoto, Japan) equipped with a flame ionization detector (GC-FID) and Rxi-5Sil M column for separation (30 m x 0.25 mm x 0.25 µm, Restek). Helium constituted the carrier gas, delivered at a column flow rate of 1.20 ml.min^{-1}. The injection volume equalled 1 µl and the temperature of injection 250 °C, while the split ratio was 1:100. A heat cycle of 40 °C for 3 minutes, followed by 70 °C.min^{-1} to 230 °C for 5 minutes was carried out for such analysis (total duration of 10.71 min). The temperature of the detector was set to 280 °C, and each sample was tested three times. The extent of ethyl lactate, ethanol, acetone and lactide in the specimens was calculated from standard calibration curves (R^2 = 0.999). Helium served as carrier gas, and all measurements were performed in triplicate.

2.3.2 GPC

Gel permeation chromatography (GPC) was employed to characterize the polymers, macromolecules and PLA residue in the mixture that contained the end product, upon completion of the degradation stage similar as in the previous work [40]. The molecular weight of the peak maxima, the number-average molecular weight, the weight-average molecular weight, and the polydispersity index of polymers were measured. Investigation took place of the product of ethyl lactate, the polymer prior to and following degradation, and of samples of dry mass of the product. A Waters HPLC system equipped with Waters differential refractometers of types e2695 and 2414 was used. The GPC system was calibrated with polystyrene standards for molecular weight within the range of 580-990500 g·mol^{-1}. The mobile phase was composed of THF (tetrahydrofuran) stabilized with butylated hydroxytoluene. Three types of columns were applied: i. a PL gel MIXED-A column (300 x 7.5 mm, 20 µm); ii.

a PL gel MIXED-B column (300 x 7.5 mm, 10 µm); and iii. a PL gel MIXED-D column (300 x 7.5 mm, 5 µm). Each product was injected at the volume of 100 µl and flow rate of 1 ml. min $^{-1}$ and 40 °C. A refractive index detector permitted detection. Before analysis commenced, each sample was dissolved in THF at the rate of 2.5 mg. ml $^{-1}$ and passed through a 0.45 µm PTFE filter. Some samples did not dissolve well, requiring the application of ultrasound. The GPC system was calibrated with polystyrene standards for molecular weight within the range of 580 and 990 500 g·mol^{-1}. All data were processed in Empower 3 software.

2.3.3 FTIR

Spectra generated by attenuated total reflectance-Fourier transform infrared spectroscopy (ATR-FTIR) were recorded for the polymer samples, and ethyl lactate product as in the previous work [40] (Nicolet iS5, Thermo Fisher Scientific, Waltham, USA). The unit was fitted with a Germanium crystal to discern how chemical bonds had structurally altered under the PLA chemical recycling conditions. The Nicolet device was set to the range of 600–4000 cm^{-1} and the resolution of 4 and 64 scans, with subsequent analysis occurring in OMNIC software (Thermo Fisher Scientific, Waltham, USA) of the product and specimens of it as dry mass, as well as the polymeric materials before (pure polymers) and after degradation (non-disappeared part).

2.3.4 Thermal analysis (DSC and TGA)

Differential scanning calorimetry (DSC) on a DSC1 STAR system (Mettler Toledo, Switzerland) and thermal gravimetric analysis (TGA) were used to assess thermal stability and structural features, of polymeric materials (named PLA-A, PLA-B-F), following the procedure described in [40]. The degree of crystallinity χ_c (%) was calculated via Equation 3[40], where ΔH^0_m constitutes the tabulated heat of fusion for the theoretically 100% crystalline PLA homopolymer (93.1 J·g^{-1}); [33,42]. This facilitated determination of the temperatures for melting point, glass transition and crystallization. Investigation of the polymer prior to and following degradation involved adding samples of ca 5 mg into aluminium pans, which were inserted into the measuring cell afterwards. Measurements were taken under a nitrogen flow rate of 50 ml.min^{-1}. A heating and cooling cycle of 10 °C.min^{-1} was applied, initially rising from 25 °C to 180 °C. This upper limit was maintained for 5 minutes before cooling transpired to -35 °C, with 5 minutes of isotherm at this temperature. A second heating scan followed, from -35 °C to 250 °C. The glass transition temperature (T_g) was determined from the thermograms as that of the midpoint of increment in heat capacity. Measurements for points of cold- and hot-crystallization exotherm and melting endotherm (T_{cc}, T_c and T_m, respectively), and enthalpies of physical transformation (ΔH_{cc},

ΔH_c and ΔH_m) of the PLA matrix were evaluated from peak maxima and the linear integration of peaks. A waxy sample underwent an initial heating cycle from 25 °C to -65 °C, with this lower temperature being maintained for 5 minutes prior to an increase to 180 °C [33,42]. The samples of TGA analysed were prepared in an identical manner to those intended for DSC [43–45]. For thermal analyses, all samples, whether granules, filaments, films, woven stack, laminate, or sackcloth, were cut into slices to ensure that the sample compactly covered the bottom of the crucible. This guaranteed the planarity and parallel orientation of the sample during measurement, enabling efficient heat transfer.

The degree of crystallinity χ_c (%) was calculated according to Equation 3 below:

$$\chi c = \frac{\Delta H_m - \Delta H_c}{\Delta H^0_m} x\, 100\,\% \quad (3)$$

where ΔH_m is the heat of fusion, ΔH_c represents cold-crystallization enthalpy ($J \cdot g^{-1}$) and ΔH^0_m is the tabulated heat of fusion for the theoretically 100% crystalline PLA homopolymer (93.1 $J \cdot g^{-1}$) [33,42].

2.3.5 X-ray diffraction

Powder and dry-mass samples of PLA for XRD (X-ray diffraction) were tested in a Rigaku Mini-Flex 600 diffractometer equipped with a CoKα (ʎ = 1.7889 Å) X-ray tube (40 KV, 15 mA); [40]. The measurement was performed in region 3-90° 2 theta with the scanning step of 0.2° and scanning rate 10°/min. Data processing was carried out in triplicate in Rigaku PDXL2 software and the PDF2 database by ICDD. For samples B and F, 1 g of material was dissolved in 1 mL of chloroform. The resulting slurry was deposited on the sample holder, and diffractograms were recorded after solvent evaporation.

2.3.6 Elemental analysis

Elemental analysis by energy dispersion X-ray spectrophotometry (EDX-XRF) was employed to check the absence of metallic or mineral elements as in the previous work [40], whereby a silicon drift detector measures the energy of the photons, resulting in a histogram that represents the distribution of X-rays with respect to power (corresponding to the amounts of the tested elements). The ethyl lactate products underwent direct analysis without dilution in an ARL Quant´EDX-XRF analyser (Thermo-Fischer Scientific). Such investigation can permit identification of more than 60 elements. Samples were placed in a Teflon cup (ca 3 g) and sealed with a microcellulose film, prior to being placed in the autosampler. Each specimen was analysed twice. Samples

were evaluated by a selected method, specifically “Any Sample Air” in Unpiquant software, which estimated the amount of elements present in mass percent (% w/w).

2.3.7 Statistical analysis

Every measurement was taken a minimum of three times in this study. The reported RSD values represent the relative standard deviation calculated from at least three measurements, providing an estimate of experimental variability, as reflected in error bars or table values. Statistical comparisons were provided by one-way analysis of variance (ANOVA), and differences were considered significant at $P < 0.05$, OriginPro 2024 SR1, OriginLab Corporation, Massachusetts USA.

2.3.8 Evaluation of degradation kinetics

The degradation kinetics were analysed using an integrated pseudo-first-order rate equation *(4):*

$$\ln(1-X) = -k \cdot t$$

(4)

where *X* represents the conversion of PLA, *t* denotes the reaction time, and *k* corresponds to the apparent pseudo-first-order rate constant. The kinetic constant k was expressed as *(5)*:

$$k = \frac{-\ln(1-X)}{t}$$

(5)

3. Results

3.1 Decomposition of mixed PLA waste materials in relation to its conversion to EL

The conditions adopted for PLA decomposition by solvolysis were in accordance with those optimized by Domincova Bergerova et al., Majgaonkar et al., Leibfahrt et al. [32,33,40]. Solvolysis was therefore carried out at 70 °C for up to 2 hours, using a 1:2 ratio of acetone to ethanol in the presence of the TBD catalyst. These conditions were selected based on previous optimization studies by Domincova Bergerova et al. [40] Testing involved several mixed waste materials (PLA-B, PLA-F) and the pure PLA granulate (PLA-A) for the sake of comparison (Table 1). The input amount of PLA material and decomposition time varied depending on material form, composition, reflecting differences in degradation extent and ethyl lactate formation (Table 2, Figure 1).

Table 2 Reaction parameters of solvolysis and data on sample and product decomposition

Sample	specification	input amount (g)	degradation (%)	time (min)	c ($g \cdot L^{-1}$)[a]	c ($g \cdot L^{-1}$)[b]	$X_{(EL)}$ (%)
PLA-A	granules	40	100.00	120	362.00	968.00	98.80
PLA-B	filaments	40	95.00	120	268.52	631.40	70.24
PLA-C	foil	10	68.75	60	227.40	307.40	37.29
PLA-D	woven stack	10	100.00	30	80.87	884.11	89.68
PLA-E	sackcloth	10	93.00	120	38.37	797.32	81.51
PLA-F	tea bags	10	61.00	120	3.82	24.64	26.87

Conditions: 70°C; 2 wt% TBD; ratio of 1: 2 sol-nuc (acetone - ethanol) in a 500-mL reaction flask

c ($g \cdot L^{-1}$)[a] - concentration of the ethyl lactate product following the reaction and prior to cleaning

c ($g \cdot L^{-1}$)[b] - [the] concentration of the ethyl lactate product after cleaning using vacuum evaporator

$X_{(EL)}$ – PLA conversion to EL

RSD of concentration measurements: 4.8 ± 0.4% (three or more measurements, no statistically significant differences were observed between replicate measurements, $P > 0.05$)

The degree to which the PLA in the samples decomposed reflected its composition. Complete decomposition (100%) was observed solely in specimens of the pure polymer (PLA-A) and PLA-based woven stack (PLA-D), both with a high proportion of polylactic acid at least 98 wt%. The PLA filament (PLA-B) and sackcloth (PLA-E) samples also decomposed to a great extent, wherein the polymer component was still high (> 90 wt%), although they also contained admixtures of additives which could not be removed by the solvolysis reaction (ca 5-7 wt%). The PLA film (PLA-C) and tea bags (PLA-F) exhibited decomposition below 70%, due to the presence of non-PLA components, such cellulose in PLA-F or high filler content (> 2%) in PLA-C. These specimens exhibited lower degradability compared to other samples, consistent with their higher content of non-PLA components. The degree of decomposition was directly correlated with the conversion of PLA to ethyl lactate, the main product of solvolysis (Table 2, Figure 1). The mass balance was evaluated by comparing the initial PLA content with the recovered solid residue after filtration, confirming that incomplete depolymerization corresponded to the presence of non-reactive components. In this regard, the higher the degree of decomposition, the greater the conversion of PLA to ethyl lactate, reflecting the higher accessibility of reactive ester bonds within the PLA matrix. To obtain a product of the highest purity, the method of purification on a vacuum evaporator from residual solvents was chosen (Table 2), [40].

For samples that did not undergo complete solvolysis depolymerization, the remaining solid fraction was separated by filtration after completion of the reaction, as described in the experimental methodology. This solid residue consisted predominantly of components originally present in the composite materials that were not susceptible to solvolysis, including cellulose fibers, inorganic fillers (e.g., $CaCO_3$), carbon black, and minor fractions of secondary polymers. These residual solid fractions represent potentially valuable secondary materials, which could be further utilized as cellulose-rich fillers, inorganic additives, or carbon-based materials, rather than being discarded as waste. The recovery of this fraction reflects the partial decomposition of the PLA matrix in these materials and the persistence of non-reactive or thermally more stable constituents.

The extent of PLA degradation ($D_{(PLA)}$) does not always correspond directly to the conversion to ethyl lactate ($X_{(EL)}$), as additives in the original material can reduce product formation even when the polymer matrix is substantially decomposed [33,40]. These additives can impair product quality and, even after purification, may lead to a decreased amount of the final product (e.g. PLA-B; Figure 1, Table 2).

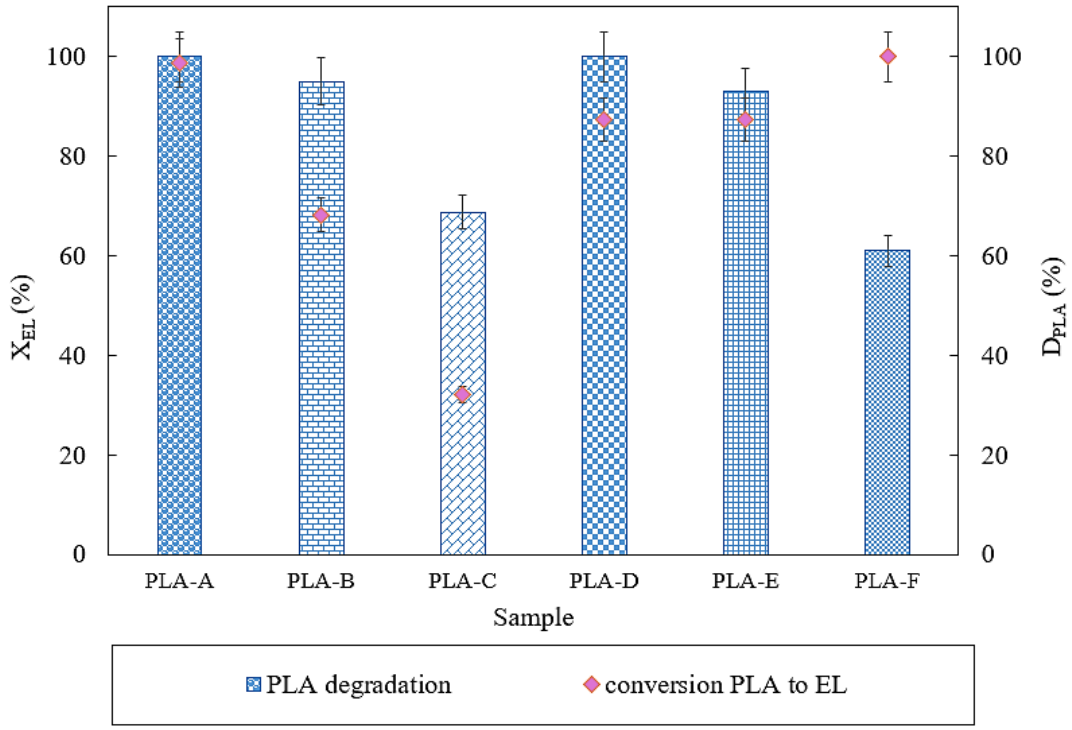

Figure 1 Effect of solvolysis on mixed PLA materials (A–F), showing polymer degradation and PLA conversion to ethyl lactate under identical reaction conditions. RSD: 5.0 ± 0.5% for polymer degradation and 2.1 ± 0.3% for polymer conversion (at least three measurements); no statistically significant differences were observed between replicate measurements ($P > 0.05$).

The course of decomposition for the individual samples, in relation to PLA conversion to ethyl lactate, is shown in Figure 2. PLA-A showed a slower increase in polymer conversion during the first 120 minutes compared to PLA-B, PLA-C, PLA-D. Once complete decomposition had occurred, ethyl lactate of very high purity and yield (up to 900 $g \cdot L^{-1}$, 98%) was obtained after solvent removal using a vacuum evaporator [40]. The conversion of PLA to ethyl lactate increased proportionally with increasing PLA content in the respective material**,** at the expense of additives and impurities. The lowest amount of ester product was observed for PLA-F**,** in which the natural polymer fraction (cellulose) comprised at least 50% of the sample**; t**his specimen also exhibited the lowest degree of decomposition (Figure 1, Table 2).

The conversion of PLA to ethyl lactate (X_{PLA}) was calculated based solely on the PLA fraction in the composite materials, excluding inert fillers and non-reactive components. This approach reflects the true chemical conversion of PLA, independent of the total composite mass. For cellulose-rich composites (e.g., PLA-F), this calculation reveals a high conversion of the PLA fraction, despite a low absolute ethyl lactate amount due to content of non-reactive cellulose (Table 2).

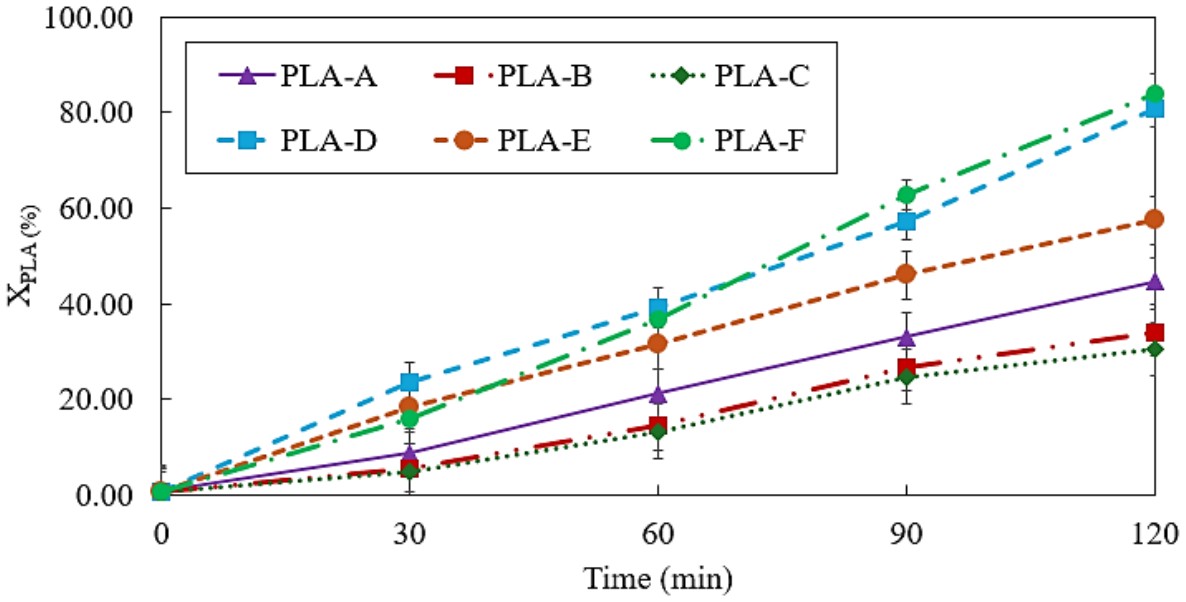

Figure 2 Effect of solvolysis time on the conversion of PLA to ethyl lactate, calculated with respect to the PLA fraction in the composite materials, RSD: 5.1 ± 0.3% (three or more measurements); PLA-D at 120 min showed a significant difference observed between replicate measurements ($P < 0.05$)

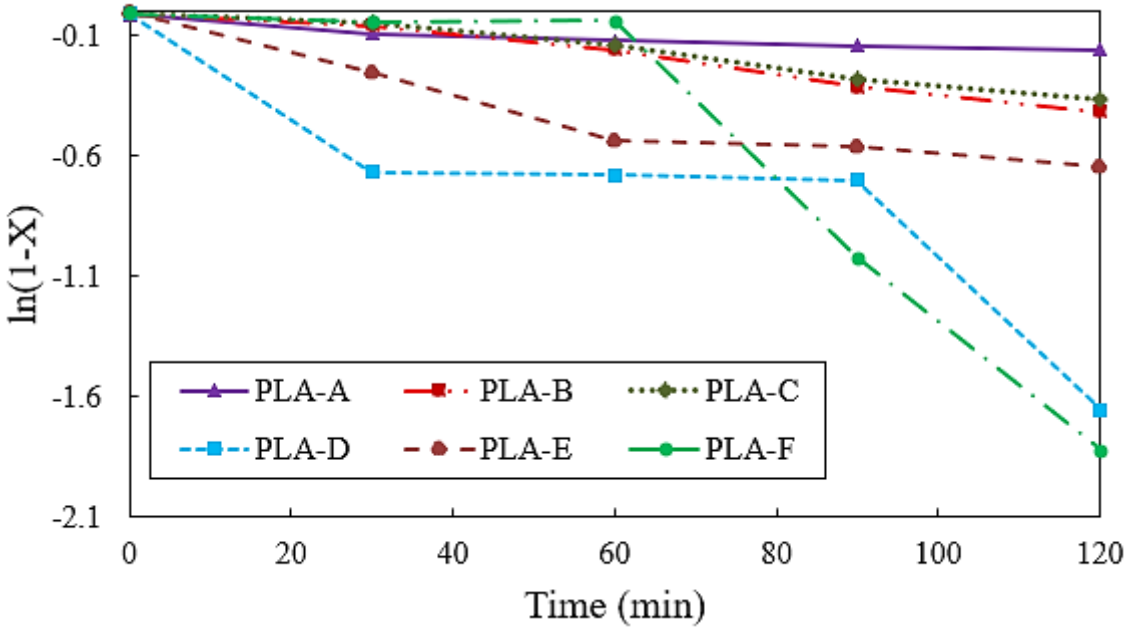

Figure 3 Kinetic analysis of PLA conversion to ethyl lactate during solvolysis, based on pseudo-first-order behaviour

Table 3 Kinetic parameters derived from the pseudo-first-order model

Sample	**−k (x 10^{-3} min^{-1})**	**ln(1−X) at 120 min (x 10^{-3})**	**t_{95} (min)**	**t_{99} (min)**
PLA-A	−1.154	−158.996	2597	3991
PLA-B	−3.573	−415.515	838	1289
PLA-C	−3.159	−364.131	948	1458
PLA-D	−1.109	−1653.912	270	415
PLA-E	−5.291	−644.167	566	870
PLA-F	−15.369	−1821.394	195	300

Since complete conversion (X = 1) would theoretically require infinite time for first-order kinetics, characteristic times corresponding to 95% and 99% conversion (t_{95} and t_{99}) were calculated instead of t_{100}. Characteristic times (t_{95} and t_{99}) were calculated from the pseudo-first-order equation $t = -\ln(1-X)/k$.

Kinetic analysis was performed assuming first- and second-order reaction models (Table 4) to compare depolymerization behavior. Linearization using the first-order equation, ln(1 − X) = −kt, gave good correlations for most samples (R^2 = 0.80–0.98). The second-order model did not improve the fit and showed lower R^2, especially for rapidly converting samples (PLA-D and PLA-F).

As shown in Figure 3, the linear relationship observed for ln(1−X) versus time suggests that the depolymerization behaviour can be reasonably described by a pseudo-first-order kinetic model. Therefore, suggesting that the rate is mainly governed by a single dominant mechanism, such as preferential degradation of amorphous regions. This approach accounts for the heterogeneous nature of the PLA materials. Deviations from ideal linearity were observed for PLA-D and PLA-F, likely due to heterogeneous structure and changes in accessibility of reactive sites during degradation, which may be influenced by the presence and nature of fillers and additives [16]. In PLA-F, the high cellulose content (>50 wt%) hinders solvent access to the embedded PLA, slowing depolymerization of the remaining fraction. In PLA-D, the woven textile structure combined with minor fillers creates heterogeneity, causing uneven reaction rates across the material. The applied kinetic models provide apparent rate constants rather than intrinsic kinetic parameters. The higher rate constant for PLA-F may reflect enhanced ethanol penetration and greater surface accessibility due to cellulose fibers.

Table 4 Apparent rate constants (k) and coefficients of determination (R^2) for pseudo-first-order and second-order kinetic models of PLA degradation.

Sample	**k (x 10^{-3} min^{-1}) 1^{st} order**	**R^2 (1^{st} order)**	**k (x 10^{-3} min^{-1}) 2^{nd} order**	**R^2 (2^{nd} order)**
PLA-A	1.154	0.886	1.262	0.900
PLA-B	3.573	0.975	4.411	0.962
PLA-C	3.159	0.973	3.803	0.963
PLA-D	11.089	0.801	28.359	0.691
PLA-E	5.291	0.894	7.549	0.923
PLA-F	15.369	0.802	40.262	0.727

The pseudo-first-order model provided consistently higher or comparable R^2 values compared to the second-order model for all PLA samples (Table 4), indicating its superior suitability for describing the degradation kinetics.

The degradation behaviour of PLA observed in this study is consistent with findings reported in previous work [40] for pure PLA samples, where similar trends in thermal decomposition and product distribution were noted. Compared to previous reports [32,33], the present approach achieved high depolymerization efficiency under milder reaction conditions, offering advantages such a lower reaction temperature, use of non-toxic reagents, and greater initial material quantities. Nevertheless, limitations such as slower kinetics or sensitivity to feedstock purity should be addressed in future work to enhance practical applicability. Overall, the results indicate that

composite content and material form primarily determine depolymerization efficiency and kinetic behavior under comparable solvolysis conditions.

3.2 Characterization of the decomposition behaviour of mixed PLA waste samples

3.2.1 Determination of the molecular weights (M_w) of the polymer materials

Molecular weight (Mw) was determined for the original materials prior to solvolysis and for the residual polymer after the reaction using gel permeation chromatography (GPC) (Table 5).

Table 5 Molecular weights (Mw) of PLA samples before and after solvolysis; RSD: 4.9 ± 0.5% (three or more measurements), no statistically significant differences were observed between replicate measurements ($P > 0.05$)

Sample	**M_w (kDa)[a]**	**M_w (kDa)[b]**	**PDI (-)[a]**	**PDI (-)[b]**
PLA-A	187	/	3.66	/
PLA-B	171	11	2.33	1.76
PLA-C	103	22	2.82	2.28
PLA-D	108	/	2.72	/
PLA-E	126	15	3.82	1.11
PLA-F	45	6	1.97	1.22

[a] – prior to commencement of the solvolysis process

[b] – after completion of the solvolysis process

For PLA-A and PLA-D, total decomposition prevented determination of Mw values, as no residual polymer remained. The molecular weights of samples diminished in parallel with the degree of polymer decomposition (PLA-B, C, E). PLA-F initially had a molecular weight of 45 kDa, which decreased to 6 kDa after degradation, indicating extensive PLA degradation, with the residual fraction primarily consisting of cellulose and low-molecular-weight fragments [33,40,46].

These results confirm that molecular weight reduction is consistent with the observed degradation trends and supports the interpretation of compositional effects on solvolysis efficiency.

3.2.2 Thermochemical characterization of tested materials

DSC and TGA were employed to characterize the thermal behavior of PLA materials before and after solvolysis, in order to evaluate the effects of additives on solvolysis treatment on crystallinity and thermal stability of materials.

3.2.2.1 Characterization of the thermal behaviour of materials using DSC

DSC analysis revealed variations in melting temperatures and degrees of crystallinity among the original PLA materials, their dry matter after dissolution in chloroform, and the residues obtained after solvolysis. The dissolution of the original materials in chloroform was performed to dissolve the PLA matrix and additives, resulting in a more homogeneous and predominantly amorphous material, and enabling a clearer interpretation of the DSC thermal transitions.

Although the differences between the original and dissolved samples in terms of melting temperatures and degrees of crystallinity were relatively small, measurable variations were observed, as reflected by the Tm and χc values listed in Table S1 (Supplementary Information). The observed thermal behaviour was influenced by the presence of fillers and additives, manifested by shifts in Tg, cold crystallization, and changes in χc, which help rationalize differences in depolymerization performance. DSC was used mainly to rationalize differences in degradation behaviour, while detailed thermal parameters are provided in the Supplementary Information (Chapter SI 1, Figure S1–S3).

In line with these DSC observations, thermal stability was further evaluated by TGA.

3.2.2.2 Thermal stability and degradation behaviour of materials using TGA

Thermal stability and degradation behaviour of the PLA materials before and after solvolysis were evaluated by thermogravimetric analysis (TGA), with the onset of decomposition defined as a 5% mass loss (Figures 4 and 5).

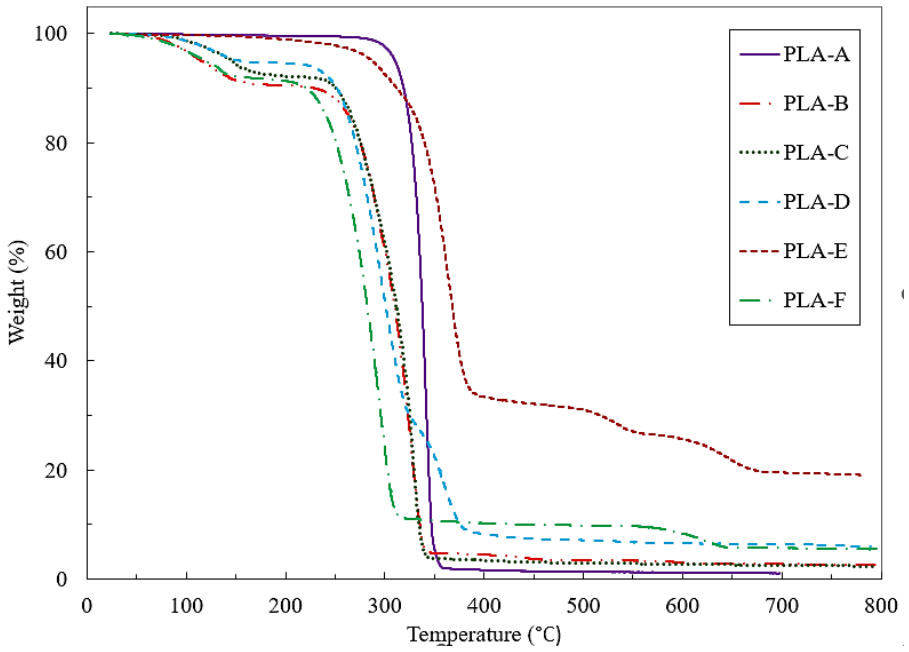

Figure 4 TGA curves of the input PLA (A-F) samples

Figure 4 shows the TGA curves of the original PLA materials (PLA-A–F). A detailed sample-specific interpretation of degradation stages and quantitative residue analysis is provided in the Supplementary Information (Section SI 2). All samples exhibited an initial mass loss below 250 °C, commonly attributed to the presence of moisture and/or low-molecular-weight components [42,47–52] . The pure PLA-A sample underwent a single-step thermal degradation process, with decomposition occurring mainly between 300-350 °C and an onset temperature of approximately 305 °C, consistent with the reported thermal behaviour of neat PLA [32,33,35,36].

In contrast, PLA materials containing fillers and additives exhibited earlier degradation onsets and more complex, multi-step decomposition profiles. In particular, the presence of calcium carbonate ($CaCO_3$) led to a reduction in thermal stability compared to pure PLA, which has been attributed to the catalytic effect of mineral fillers on the depolymerization of PLA ester bonds [15,24–26,29–31]. The incorporation of plasticizers further contributed to a decrease in decomposition temperature, in agreement with literature reports on plasticized PLA systems [24,37,38]. Conversely, samples containing a higher proportion of cellulose exhibited enhanced thermal stability, confirming the stabilizing effect of cellulose on polymer matrices reported previously [53].

Overall, thermal degradation of PLA occurred predominantly within the temperature range of 150–400 °C (the lower onset being associated with the presence of plasticizers and low-molecular-weight components),

corresponding to chain scission degradation mechanisms [36,54]. The observed differences among the samples reflect variations in additive content, crystallinity, and structural characteristics of the PLA matrices.

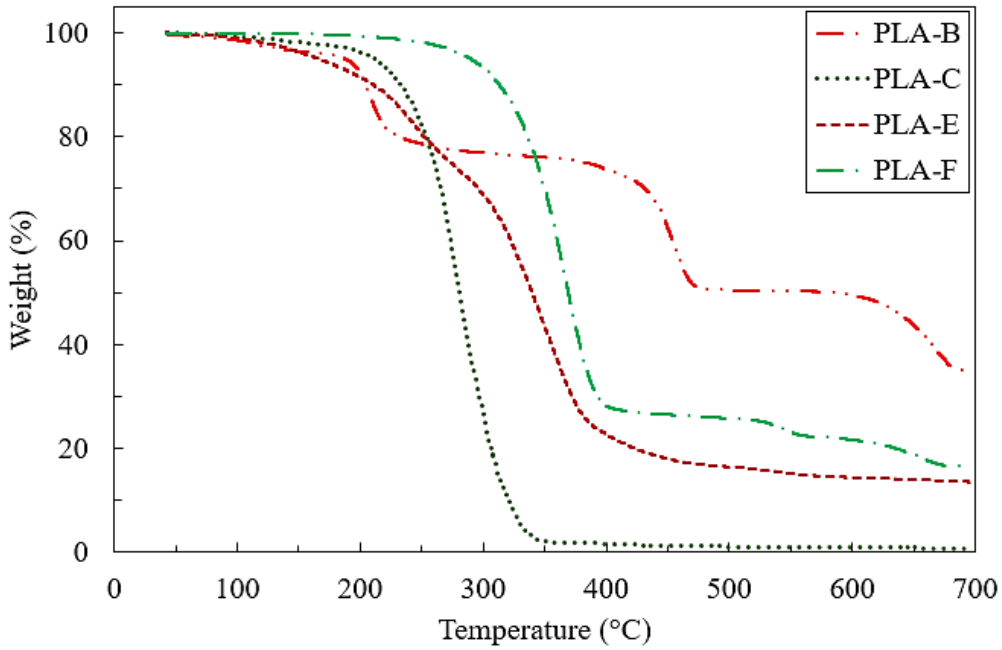

Figure 5 TGA curves of the PLA (B, C, E, F) samples after solvolysis

Since PLA-A and PLA-D were fully decomposed during solvolysis, they were not further evaluated by TGA. The post-solvolysis samples generally exhibited lower decomposition onset temperatures and higher relative inorganic residue contents, reflecting the removal of the PLA matrix and the enrichment of inorganic components, particularly $CaCO_3$ [4,24,25]. A comprehensive discussion of the individual degradation steps and residual mass fractions is given in the Supplementary Information (Section SI 2). In materials with higher cellulose content, increased resistance to thermal degradation was retained even after solvolysis, in agreement with DSC observations [53].

Taken together, TGA confirmed that the thermal stability and degradation behaviour of the investigated PLA materials were strongly influenced by the presence of fillers, plasticizers, and secondary polymeric components. These findings are consistent with the DSC results and demonstrate the combined effect of material composition and solvolysis treatment on the thermal response of PLA. Detailed sample specific TGA interpretation and quantitative residue analysis are provided in the Supplementary Information (Chapter SI 2).

The presence of a residual solid fraction after solvolysis is further supported by DSC and TGA analyses, which reveal thermal transitions and degradation profiles corresponding to non-PLA components. In particular, cellulose-rich samples and materials containing inorganic fillers exhibit characteristic thermal stability and residual mass, confirming that these components persist after selective depolymerization of the PLA matrix.

3.2.3 Chemical structures of tested materials

The investigated polymers were analysed by XRD and ATR-FTIR, with XRD used primarily to identify crystalline phases. The diffractograms of each PLA material are detailed in Figure 6.

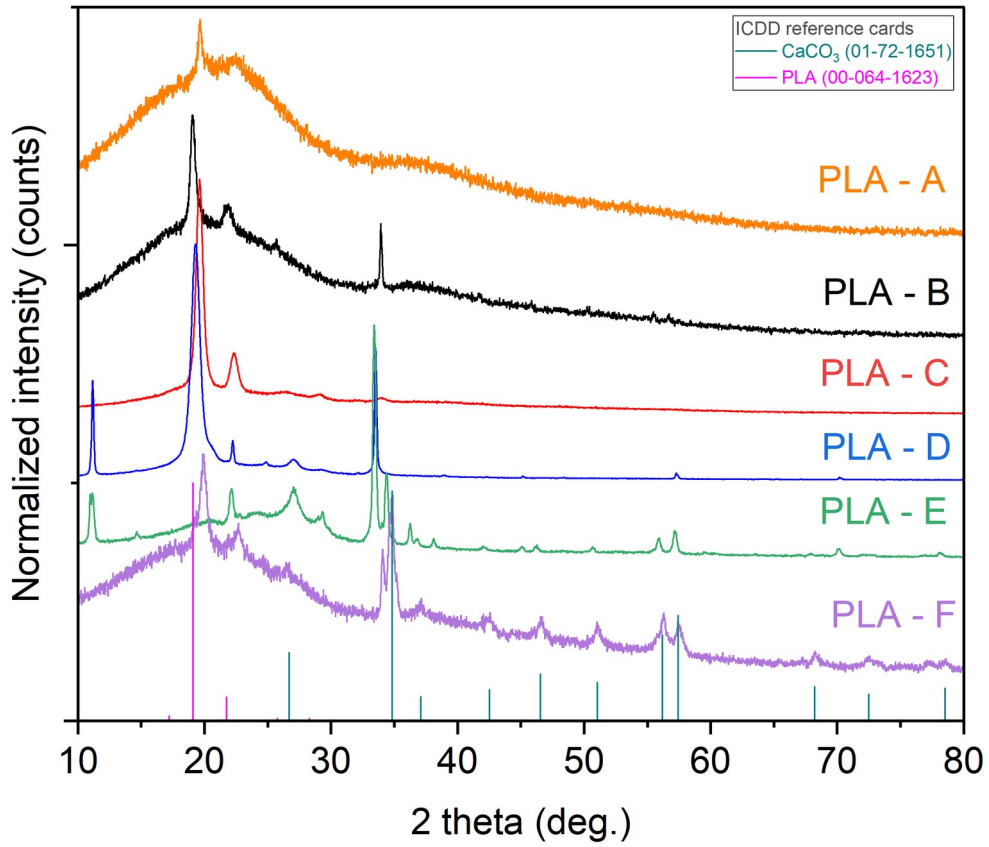

Figure 6 Powder X-ray diffractograms for the dry mass of PLA (A-F) with reference cards: ICDD PDF (00-064-1623, and 01-072-1651). Patterns are vertically offset for clarity

Figure 6 presents X-ray diffraction patterns for the PLA materials as dry mass (PLA-A-F). XRD revealed diffraction lines between 16° and 23° 2 theta, and less prominent diffractions between 26°–40°. Diffractions appearing at ~12–18° and in the range 40-70° 2 theta suggest the presence of additional phases associated with additives or secondary polymer matrices. As illustrated in Figure 6, diffraction patterns were matched to PLA

ICDD PDF reference card with number 00-064-1623. The slight shifts in the PLA diffraction peaks are most likely caused by inhomogeneous morphology and differences in the macroscopic structure of the samples, which can lead to small variations in their positioning on the sample holder. Based on the diffractograms, the components could be assigned. The diffractograms indicate variations in filler content and material form among the investigated samples (granules, foils, woven stack). After dissolution of PLA (A-E) samples in chloroform and solvent evaporation, the materials exhibited reduced crystallinity, reflecting disruption of the original polymer morphology (see the DSC results in Supplementary information, Table S1). The PLA-A pure polymer exhibited predominantly amorphous character with only weak diffraction maxima (Table S1, Figure 6). Characteristic broad reflections typical of semi-crystalline PLA were observed in the region of approximately 16-23 °. XRD analysis demonstrated the presence of additives in sample PLA-B, PLA-E compared with pure PLA-A. PLA-D displayed additional diffraction peaks at approximately 12°, 35°, 58° and 70°, indicating the presence of secondary polymeric components or additives (Table 1). PLA-E contained distinct peaks in the regions of 10°, 35°, 58° and 70°, but differed from those in the case of PLA-D due to double peaks in the area 55-58°. These differences suggest the presence of additional polymeric components in sample E (for example some cellulose), consistent with the compositional data in Table 1. Based on the XRD patterns, the PLA samples denoted as B, E, F contain an inorganic filler $CaCO_3$ (a slight peak appears at ca 34-35 °), assigned to ICDD PDF card 01-072-1651. Inorganic fillers (e.g., $CaCO_3$) were identified in PLA-C, while additional features potentially associated with carbon black were observed in PLA-B and PLA-E (Figure 6, Table 1). In PLA-F, cellulose peaks may overlap with PLA reflections in the 20–22° region, making unambiguous identification difficult. According to the literature, peaks for PLA identification are in the area at 18 – 22°, which corresponds to the XRD patterns observed for the examined materials (PLA-A-F) [16].

The ATR-FTIR spectra of all PLA-based composites were recorded to verify the presence of characteristic functional groups and assess any structural modifications induced by additives. The spectra confirm the expected chemical structures, and no unexpected peaks were observed. FTIR spectra are provided in the Supplementary Information (SI 3; Figure S4–S9).

3.2.4 Elemental analysis of PLA composites

Elemental analysis was performed to determine the composition of the composites and quantify the content of inorganic fillers and additives. The results indicate good agreement with nominal formulations and confirm the

successful incorporation of all components. Elemental composition of the composites is summarized in Table S4 (Supplementary information, Chapter SI 4).

Overall, the main structural and compositional characteristics of the composites confirm successful incorporation of additives and support the observed trends in solvolysis depolymerization efficiency.

3.2.5 Limitations and Future Directions

Despite the promising results obtained in this study, several limitations must be acknowledged. The solvolysis conditions (using acetone as the solvent, ethanol as the nucleophile, a single organic catalyst, and fixed temperature/time parameters) were not optimized for each material type, which may influence degradation efficiency across different formulations. However, the conditions were based on an optimized procedure described by Domincová Bergerová et al. [40], originally developed for PLA materials, where high product yield and purity were demonstrated. Moreover, only five PLA-based materials were tested. While representative of common additive types, they do not encompass the full diversity of commercially available PLA composites or post-consumer waste. The mechanistic role of individual additives on the solvolysis process was inferred from overall trends rather than investigated directly at the molecular level. In addition, the study did not assess environmental impacts or economic aspects, which are critical for evaluating the feasibility of large-scale application. The applied solvolysis conditions were comparatively mild and based on the use of environmentally benign reagents relative to previously reported methods [11,15] .

Future work should address these limitations by expanding the scope to include industrial waste streams and post-consumer PLA composites. Systematic optimization of solvolysis parameters and kinetic modelling could improve product yield and overall process efficiency. In-depth studies on additive–matrix interactions during solvolysis, including monitoring and molecular-level analysis, are needed to better understand the degradation mechanisms. Furthermore, techno-economic and life cycle assessment will be essential for validating the sustainability and scalability of this recycling method.

4. Conclusion

Compared with our earlier study on virgin PLA [40], this work demonstrates that the efficiency of solvolysis depolymerization of poly(lactic acid) is primarily governed by the form of the material (granules, filaments, textiles, laminates) and the presence and nature of industrial additives in the PLA composites. Granular and

woven textile materials with high PLA content (≥90 wt%) exhibited complete or near-complete depolymerization, whereas laminated and cellulose-rich composite structures showed reduced conversion due to limited accessibility of ester bonds within the heterogeneous matrix. Although additives influence crystallinity and thermal stability, the results clearly show that compositional parameters decisively determine depolymerization performance and product recovery.

Commonly used inorganic fillers and modifiers, such as calcium carbonate at low content (<1.5 wt%), carbon black, and plasticizers, did not significantly hinder solvolysis and enabled high PLA conversion to ethyl lactate (up to 98%). In contrast, high additive contents, particularly cellulose-rich matrices (>50 wt%), substantially reduced depolymerization efficiency and PLA conversion to ethyl lactate, identifying cellulose-rich matrices as a practical composition limit for solvolysis recycling under the applied conditions. This effect is likely due to changes in accessibility of reactive ester bonds and altered degradation kinetics caused by high cellulose content. Minor amounts (<1 wt%) of secondary polymers, such as DETPE or PBAT, showed no significant impact on the solvolysis process. These findings indicate that solvolysis performance is governed not only by additive content but also by additive chemical nature and its influence on polymer architecture, crystallinity, and accessibility of ester bonds within heterogeneous composite matrices.

All investigated PLA-based materials underwent substantial depolymerization under the applied reaction conditions, despite pronounced structural differences confirmed by XRD and ATR-FTIR analyses. Differences in thermal degradation onset were attributed to variations in molecular weight (M_w), glass transition (T_g), melting temperature (T_m), and composite formulation, consistent with the observed degradation behavior.

The novelty of this work lies in extending solvolysis recycling from studies on virgin PLA to commercially relevant composites and in systematically evaluating how industrial additives influence depolymerization efficiency and ethyl lactate recovery. Detailed thermal analyses (DSC and TGA) support the interpretation of degradation mechanisms and material stability, aiding process control and scalability considerations. Importantly, the recovered solid residues represent a potentially valuable secondary material stream. Depending on their PLA/non-PLA composition, these fractions may be further utilized, for example as cellulose-rich fillers, inorganic additives, or carbon-based materials, rather than being treated as waste. This aspect highlights an additional advantage of solvolysis within a circular economy framework, where both the depolymerized PLA and the non-reactive composite constituents can be separated and valorized.

Overall, the demonstrated solvolysis approach represents a promising pathway for the chemical recycling of additive-rich PLA materials into high-purity ethyl lactate. Future work should focus on optimizing reaction parameters, solvent recovery, and techno-economic assessment to further support industrial implementation.

CRediT authorship contribution statement

Domincova Bergerova Eva: Conceptualization, data curation, investigation, methodology, project administration, validation, visualization, roles/writing - original draft; **Sedlarik Vladimir:** supervision, writing - review & editing, formal analysis, funding acquisition; **Cisar Jaroslav, Strasakova Monika, Uhercova Simona, Hanusova Dominika, Dusankova Miroslava and Skoda David:** methodology, investigation.

Declaration of competing interests

The authors declare that they have no conflict of interests.

Acknowledgements

This work was supported from the European Just Transition Fund within the Operational Programme Just Transition under the aegis of the Ministry of the Environment of the Czech Republic, project CirkArena number CZ.10.03.01/00/22_003/0000045 and the Ministry of Education Youth and Sports of the Czech Republic, Operational Programme Johannes Amos Comenius OP JAC “Application potential development in the field of polymer materials in the context of circular economy compliance (POCEK)”, number CZ.02.01.01/00/23_021/0009004. Authors are further grateful for co-funding from the development process of Centre of Polymer Systems, Tomas Bata University in Zlín, programme DKRVO (RP/CPS/2024-28/002) and (RP/CPS/2024-28/007) supported by the Ministry of Education Youth and Sports of the Czech Republic.

Data availability

Data will be made available on request.

Reference

[1] A. Samir,, F.H. Ashour,, A.A.A. Hakim,, M. Bassyouni, Npj Mater. Degrad. 6(1) (2022). 10.1038/s41529-022-00277-7.

[2] A. Künkel,, J. Becker,, L. Börger,, J. Hamprecht,, S. Koltzenburg,, R. Loos,, M.B. Schick,, K. Schlegel,, C. Sinkel,, G. Skupin,, M. Yamamoto, Ullmann's Encyclopedia of Industrial Chemistry, Wiley-VCH Verlag GmbH & Co. KGaA, Weinheim, Germany, 2016, pp. 1–29.

[3] B. Ghanbarzadeh, Biodegradable Polymers, Vol. 16, 2024.

[4] M.N. Siddiqui,, H.H. Redhwi,, A.A. Al-Arfaj,, D.S. Achilias,, M.N.; Siddiqui,, H.H.; Redhwi,, A.A.; Al-Arfaj,, D.S. Achilias, Sustain. 2021, Vol. 13, Page 10528 13(19) (2021) 10528. 10.3390/SU131910528.

[5] A. Behrens, Time to connect the dots: What is the link between climate change policy and the circular economy?, Brussels, 2016.

[6] M.E. González-López,, A.S. Martín del Campo,, J.R. Robledo-Ortíz,, M. Arellano,, A.A. Pérez-Fonseca, Polym. Degrad. Stab. 179 (2020). 10.1016/j.polymdegradstab.2020.109290.

[7] X. Liu,, S. Khor,, E. Petinakis,, L. Yu,, G. Simon,, K. Dean,, S. Bateman, Thermochim. Acta 509(1–2) (2010) 147–51. 10.1016/J.TCA.2010.06.015.

[8] M. Schneider,, N. Fritzsche,, A. Puciul-Malinowska,, A. Baliś,, A. Mostafa,, I. Bald,, S. Zapotoczny,, A. Taubert, Polymers (Basel). 12(8) (2020). 10.3390/POLYM12081711.

[9] M. Zdanowicz,, M. Mizielińska,, A. Kowalczyk, Polymers (Basel). 16(14) (2024). 10.3390/polym16141954.

[10] E. Balla,, V. Daniilidis,, G. Karlioti,, T. Kalamas,, M. Stefanidou,, N.D. Bikiaris,, A. Vlachopoulos,, I. Koumentakou,, D.N. Bikiaris, Polymers (Basel). (2021). 10.3390/polym13111822.

[11] A. Carné Sánchez,, S.R. Collinson, Eur. Polym. J. 47(10) (2011) 1970–6. 10.1016/j.eurpolymj.2011.07.013.

[12] L. Alaerts,, M. Augustinus,, K. Van Acker, Sustain. 10(5) (2018). 10.3390/su10051487.

[13] L. Aliotta,, P. Cinelli,, M.B. Coltelli,, M.C. Righetti,, M. Gazzano,, A. Lazzeri, Eur. Polym. J. 93(May) (2017) 822–32. 10.1016/j.eurpolymj.2017.04.041.

[14] G. Spinelli,, P. Lamberti,, V. Tucci,, R. Kotsilkova,, S. Tabakova,, R. Ivanova,, P. Angelova,, V. Angelov,, E. Ivanov,, R. Di Maio,, C. Silvestre,, D. Meisak,, A. Paddubskaya,, P. Kuzhir, Materials (Basel). 11(11) (2018). 10.3390/ma11112256.

[15] P. Szatkowski,, J. Gralewski,, K. Suchorowiec,, K. Kosowska,, B. Mielan,, M. Kisilewicz, Materials

(Basel). 17(1) (2024) 1–18. 10.3390/ma17010022.

[16] L. Quiles-Carrillo,, N. Montanes,, D. Garcia-Garcia,, A. Carbonell-Verdu,, R. Balart,, S. Torres-Giner, Compos. Part B Eng. 147(February 2017) (2018) 76–85. 10.1016/j.compositesb.2018.04.017.

[17] R. Shorey,, T.H. Mekonnen, Int. J. Biol. Macromol. 268(P1) (2024) 131672. 10.1016/j.ijbiomac.2024.131672.

[18] S. Thumsorn,, W. Prasong,, T. Kurose,, A. Ishigami,, Y. Kobayashi,, H. Ito, Polymers (Basel). 14(13) (2022) 1–22. 10.3390/polym14132721.

[19] K.R.R. b , D.A.G. b , P.R.G. b Erwin T.H. Vink a, Polym. Degrad. Stab. (2003) 403419.

[20] Erwin T. H. VinkSteve Davies, Ind. Biotechnol. 11(3) (2015) 167–80.

[21] M.H. Rathin Datta, J. Chem. Technol. Biotechnol. (2006).

[22] J. Finnerty,, S. Rowe,, T. Howard,, S. Connolly,, C. Doran,, D.M. Devine,, N.M. Gately,, V. Chyzna,, A. Portela,, G.S.N. Bezerra,, P. McDonald,, D.M. Colbert, J. Compos. Sci. 7(4) (2023) 1–17. 10.3390/jcs7040141.

[23] R. Arrigo,, M. Bartoli,, G. Malucelli, Polymers (Basel). 12(4) (2020) 1–13. 10.3390/POLYM12040892.

[24] N.G. Betancourt,, D.E. Cree, MRS Adv. 2(47) (2017) 2545–50. 10.1557/adv.2017.473.

[25] A. Pudełko,, P. Postawa,, T. Stachowiak,, K. Malińska,, D. Dróżdż, J. Clean. Prod. 278 (2021). 10.1016/j.jclepro.2020.123850.

[26] Y. Xia,, S. Qian,, X. Zhang,, Z. Zhang,, C. Zhu, Ind. Crops Prod. 219(June) (2024) 119049. 10.1016/j.indcrop.2024.119049.

[27] D. Tonini,, P. Garcia-Gutierrez,, S. Nessi, Environmental effects of plastic waste recycling, 2021.

[28] P. Yadav,, R. Farnood,, V. Kumar, J. Environ. Chem. Eng. 9(6) (2021) 106507. 10.1016/J.JECE.2021.106507.

[29] C. Pavon,, M. Aldas,, M.D. Samper,, D.L. Motoc,, S. Ferrandiz,, J. López-Martínez, Polymers (Basel). 14(13) (2022). 10.3390/polym14132646.

[30] S. Thakur,, J. Chaudhary,, B. Sharma,, A. Verma,, S. Tamulevicius,, V.K. Thakur, Curr. Opin. Green Sustain. Chem. 13 (2018) 68–75. 10.1016/j.cogsc.2018.04.013.

[31] R. Geyer,, J.R. Jambeck,, K.L. Law, Sci. Adv. 3(July) (2017) 25–9.

[32] P. Majgaonkar,, R. Hanich,, F. Malz,, R. Brüll, Chem. Eng. J. 423 (2021). 10.1016/j.cej.2021.129952.

[33] F.A. Leibfarth,, N. Moreno,, A.P. Hawker,, J.D. Shand, J Polym Sci Part A Polym Chem 50 (2012) 4814–22. 10.1002/pola.26303.

[34] P. Majgaonkar,, R. Hanich,, F. Malz,, R. Brüll, Chem. Eng. J. 423 (2021) 129952. 10.1016/j.cej.2021.129952.

[35] F. Liendo,, M. Arduino,, F.A. Deorsola,, S. Bensaid, Powder Technol. 398 (2022) 117050. 10.1016/j.powtec.2021.117050.

[36] M.H. Azarian,, W. Sutapun, Front. Mater. 9(November) (2022) 1–17. 10.3389/fmats.2022.1024977.

[37] L.A. Román-Ramírez,, P. McKeown,, M.D. Jones,, J. Wood, ACS Omega 5(10) (2020) 5556–64. 10.1021/acsomega.0c00291.

[38] E. des Ligneris,, L.F. Dumée,, L. Kong, Environ. Nanotechnology, Monit. Manag. 13 (2020) 100297. 10.1016/J.ENMM.2020.100297.

[39] S. Ellis,, A. Buchard,, T. Junkers, Chem. Sci. 16(1) (2024) 211–7. 10.1039/d4sc05891g.

[40] E.D. Bergerova,, M. Strasakova,, J. Cisar,, T. Sopik,, M. Dusankova,, I. Vincent,, J. Klaban,, D. Hanusova,, S. Uhercova,, L. Hanykova,, V. Sedlarik, Int. J. Biol. Macromol. 302(October 2024) (2025) 140529. 10.1016/j.ijbiomac.2025.140529.

[41] J. Cisar,, P. Drohsler,, M. Pummerova,, V. Sedlarik,, D. Skoda, Polymer (Guildf). 276 (2023). 10.1016/j.polymer.2023.125943.

[42] F. Signori,, M.B. Coltelli,, S. Bronco, Polym. Degrad. Stab. 94(1) (2009) 74–82. 10.1016/j.polymdegradstab.2008.10.004.

[43] I. Velghe,, B. Buffel,, V. Vandeginste,, W. Thielemans,, F. Desplentere, Polymers (Basel). 15(9) (2023) 2047. 10.3390/polym15092047.

[44] M. Ineke Velghe, MURAKAMI, Melt Process. High-Temperature Supercond. (1993) 21–44. 10.1142/9789814335898_0003.

[45] M. Cvek,, U.C. Paul,, J. Zia,, G. Mancini,, V. Sedlarik,, A. Athanassiou, ACS Appl. Mater. Interfaces 14(12) (2022) 14654–67. 10.1021/acsami.2c02181.

[46] N. Huang,, J. Wang, J. Anal. Appl. Pyrolysis 84(2) (2009) 124–30. 10.1016/j.jaap.2009.01.001.

[47] S. Faba,, Á. Agüero,, M.P. Arrieta,, S. Martínez,, J. Romero,, A. Torres,, M.J. Galotto, Polymers (Basel). 16(6) (2024) 798. 10.3390/polym16060798.

[48] Q. Meng,, M.C. Heuzey,, P.J. Carreau, Polym. Degrad. Stab. 97(10) (2012) 2010–20. 10.1016/j.polymdegradstab.2012.01.030.

[49] C. Hopmann,, S. Schippers,, C. Höfs, J. Appl. Polym. Sci. 132(9) (2015) 1–6. 10.1002/app.41532.

[50] A.A. Cuadri,, J.E. Martín-Alfonso, Polym. Degrad. Stab. 150(January) (2018) 37–45.

10.1016/j.polymdegradstab.2018.02.011.

[51] A. Södergård,, M. Stolt, Prog. Polym. Sci. 27(6) (2002) 1123–63. 10.1016/S0079-6700(02)00012-6.

[52] H. Zou,, C. Yi,, L. Wang,, H. Liu,, W. Xu, J. Therm. Anal. Calorim. 97(3) (2009) 929–35. 10.1007/s10973-009-0121-5.

[53] T. Kato,, T. Suzuki,, T. Amamiya,, T. Irie,, M. Komiyama,, H. Yui, Supramol. Sci. 5(3–4) (1998) 411–5. 10.1016/S0968-5677(98)00041-8.

[54] F. Liendo,, M. Arduino,, F.A. Deorsola,, S. Bensaid, Powder Technol. 398 (2022) 117050. 10.1016/j.powtec.2021.117050.

[55] P.K. Mahapatro, (Lica 12) (1991).

[56] K. Gorna,, M. Hund,, M. Vučak,, F. Gröhn,, G. Wegner, Mater. Sci. Eng. A 477(1–2) (2008) 217–25. 10.1016/j.msea.2007.05.045.

[57] N. Guermazi,, N. Haddar,, K. Elleuch,, H.F. Ayedi, Polym. Compos. 37(7) (2016) 2171–83. 10.1002/pc.23396.

[58] E. de C. Nunes,, A.G. de Souza,, D. dos S. Rosa, J. Compos. Mater. 54(10) (2020) 1373–82. 10.1177/0021998319880282.

[59] F. Ippolito,, G. Hübner,, T. Claypole,, P. Gane, Polymers (Basel). 12(6) (2020). 10.3390/polym12061295.

[60] T. Thenepalli,, A.Y. Jun,, C. Han,, C. Ramakrishna,, J.W. Ahn, Korean J. Chem. Eng. 32(6) (2015) 1009–22. 10.1007/s11814-015-0057-3.

[61] M. Al-Samhan,, F. Al-Attar, Surfaces and Interfaces 31(October 2021) (2022) 102055. 10.1016/j.surfin.2022.102055.

[62] R. Auras,, B. Harte,, S. Selke, Macromol. Biosci. (2004) 835–64. 10.1002/mabi.200400043.

[63] G. Kister,, G. Cassanas,, M. Vert, Effects of morphology, conformation and configuration on the IR and Raman spectra of various poly(lactic acid)s, Vol. 39, 1998.

[64] G. Socrates, Infrared and raman characteristic group frequencies : tables and charts., John Wiley & Sons, 2007.

[65] H. Younes,, D. Cohn, Eur. Polym. J. 24(8) (1988) 765–73. 10.1016/0014-3057(88)90013-4.

[66] Z. Sun,, S. Xu,, B. Zhang,, J. Zhong,, K. Dai,, G. Zheng,, C. Liu,, C. Shen, Polymer (Guildf). 295 (2024). 10.1016/j.polymer.2024.126788.

[67] S.M. Lebedev, Int. J. Adv. Manuf. Technol. 102(9–12) (2019) 3213–6. 10.1007/s00170-019-03420-y.

[68] P. Chang,, J.Y. Kim,, K.W. Kim, Environ. Geochemistry Heal. 2005 272 27(2) (2005) 109–19. 10.1007/S10653-005-0130-7.

[69] M. Malinauskas,, A. Žukauskas,, S. Hasegawa,, Y. Hayasaki,, V. Mizeikis,, R. Buividas,, S. Juodkazis, Light Sci. Appl. (2016). 10.1038/lsa.2016.133.

[70] C.C. Lin,, S.J. Fu,, Y.C. Lin,, I.K. Yang,, Y. Gu, Int. J. Biol. Macromol. 68 (2014) 39–47. 10.1016/j.ijbiomac.2014.04.039.